A HYBRID WAVE BASED VIBRO-ACOUSTIC MODELLING TECHNIQUE FOR THE PREDICTION OF INTERIOR NOISE IN AN AIRCRAFT FUSELAGE

B. Van Genechten , D. Vandepitte , W. Desmet
K.U.Leuven, Dept. of Mechanical Engineering, Division PMA
Celestijnenlaan 300B, B-3001 Leuven (Heverlee), Belgium
email: Bert.VanGenechten@mech.kuleuven.be
url: http://www.mech.kuleuven.be/mod/wbm/

Keywords: *numerical methods, vibro-acoustics, wave based method, hybrid methods*

Abstract

This paper presents a newly developed hybrid simulation technique for interior coupled vibro-acoustic analysis, which applies a wave based model for the acoustic cavity and a finite element model for the structure. The resulting hybrid model benefits from the computational efficiency of the wave based method, while retaining the finite element method's ability to model the structural part of the problem in great detail. Application of this approach to the study of the interior noise inside a section of an aircraft shows an improved computational efficiency over classical finite element procedures and illustrates the potential of the hybrid method as a powerful tool for the analysis of coupled vibro-acoustic systems.

1 Introduction

The use of numerical models for functional performance evaluation has become common practice in industry. The most popular techniques to perform interior coupled vibro-acoustic analyses are the Finite Element Method [1] (FEM) and the Boundary Element Method [2] (BEM). These deterministic simulation techniques discretise the considered problem or its boundary into a finite number of elements. Within these elements, the dynamic response variables are described by an expansion of simple (polynomial) shape functions, which are no exact solutions of the governing differential equations. As a result, as frequency increases, the prediction accuracy of the element based models decreases, mainly due to two types of errors: interpolation and pollution errors [3]. Keeping these errors within acceptable bounds requires the use of extremely dense problem discretisations, especially at higher frequencies. This results in prohibitively large numerical models for real-life vibro-acoustic problems. As a result, the applicability of the element based techniques is limited to problems in the low-frequency range. One of the major advantages of the element based methods is their ability to model any problem, regardless of its geometrical complexity.

The Wave Based Method (WBM) [4] belongs to the family of so-called Trefftz methods [5] and has shown to be applicable for vibro-acoustic problems in the mid-frequency range [6]. This deterministic technique applies globally defined wave functions, which are exact solutions of the governing differential equations, instead of approximating shape functions, to describe the dynamic response variables. As a result, the use of very dense domain discretisations at higher frequencies is no longer required. The size of the numerical models and the required computational resources are substantially lower as compared with element based methods. Because of

the enhanced convergence properties, the WBM can be applied to low- and mid-frequency applications. A sufficient condition for convergence of the applied wave function expansions, is the convexity of the considered problem domains. Non-convex domains have to be partitioned into a number of (convex) subdomains. As a result, in order to fully benefit from the method's efficiency, only problems of moderate geometrical complexity are considered.

In recent years, combination of the geometrical flexibility of the FEM with the enhanced convergence properties of the WBM in a hybrid modelling technique has been successfully explored for uncoupled acoustic [7] and uncoupled structural problems [8]. This paper presents a newly developed hybrid simulation technique, in which a direct coupling is realised between a structural FE model and an acoustic WB model. The novel technique can be applied to vibro-acoustic problems in which a complex structure is in contact with acoustic cavity of moderate geometrical complexity. The first section of the paper describes the mathematical formulation of the novel hybrid FE-WB method. Section 3 illustrates the improved computational efficiency of the method as compared to classical FE procedures through an application study of interior aircraft noise, which has been a topic of interest in the past decades.

2 A hybrid FE-WB method for coupled vibro-acoustic problems

2.1 Problem definition

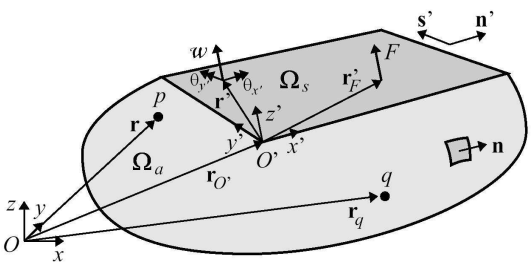

Fig. 1 A 3D coupled vibro-acoustic problem

The steady-state dynamic behaviour of a general coupled vibro-acoustic system, as shown in figure 1, is described by two physical variables: the acoustic pressure $p(\mathbf{r})$ at a position $\mathbf{r}(x,y,z)$ in the internal acoustic cavity and the combined dynamic in-plane ($w_{x'}(\mathbf{r}')$, $w_{y'}(\mathbf{r}')$) and out-of-plane deformations ($w_{z'}(\mathbf{r}')$, $\theta_{x'}(\mathbf{r}')$, $\theta_{y'}(\mathbf{r}')$) at a position $\mathbf{r}'(x',y')$ in the structural domain Ω_s. The z'-axis of the local coordinate frame (x',y',z') is normal to the structure and points away from the acoustic cavity.

The acoustic cavity V is filled with air, with ambient fluid density ρ_a and speed of sound c. An acoustic point source q at position $\mathbf{r_q}(x_q,y_q,z_q)$ within the cavity excites the fluid at circular frequency ω. Under the assumption that the fluid in the cavity behaves linear, inviscid and adiabatic, the Helmholtz equation governs the steady-state acoustic pressure $p(\mathbf{r})$ inside the cavity [9]:

$$\triangle p(\mathbf{r}) + k^2 \cdot p(\mathbf{r}) = -j\rho_a \omega q \cdot \delta(\mathbf{r}, \mathbf{r_q}) \qquad (1)$$

with $\triangle = \frac{\partial^2}{\partial x^2} + \frac{\partial^2}{\partial y^2} + \frac{\partial^2}{\partial z^2}$ the Laplacian operator, $k = \frac{\omega}{c}$ the acoustic wave number, $j = \sqrt{-1}$ the imaginary unit and δ a Dirac delta function.

Since the Helmholtz equation (1) is a second order differential equation, one boundary condition needs to be specified at each point of the boundary in order to obtain a well-posed problem. The boundary Ω_a of the acoustic domain consists of four non-overlapping parts, ($\Omega_a = \Omega_p \bigcup \Omega_v \bigcup \Omega_Z \bigcup \Omega_s$). On each of the first three parts of the boundary, Ω_p, Ω_v and Ω_Z, acoustic pressure, acoustic normal velocity and normal impedance boundary conditions are specified respectively:

$$\begin{aligned} R_p(\mathbf{r}) &= p(\mathbf{r}) - \bar{p}(\mathbf{r}) = 0, \quad \mathbf{r} \in \Omega_p \\ R_v(\mathbf{r}) &= \frac{j}{\rho_a \omega} \frac{\partial p\mathbf{r}}{\partial \mathbf{n}} - \bar{v}_n(\mathbf{r}) = 0, \quad (\mathbf{r}) \in \Omega_v \\ R_Z(\mathbf{r}) &= \frac{j}{\rho_a \omega} \frac{\partial p(\mathbf{r})}{\partial \mathbf{n}} - \frac{p(\mathbf{r})}{\bar{Z}_n(\mathbf{r})} = 0, \quad \mathbf{r} \in \Omega_Z \end{aligned} \qquad (2)$$

with $\frac{\partial}{\partial \mathbf{n}}$ the normal derivative and $\bar{p}(\mathbf{r})$, $\bar{v}_n(\mathbf{r})$ and $\bar{Z}_n(\mathbf{r})$ predefined values for the acoustic pressure, normal velocity and normal impedance, respectively.

The part Ω_s of the boundary consists of a flexible plate assembly, made of a material with density ρ_s, Young's modulus E and Poisson ratio ν.

The structure is excited harmonically by a point force F at position $\mathbf{r}'_{\mathbf{F}}(x'_F, y'_F)$. The dynamic deformations within the plates consists of two superimposed deformation fields, which are mutually coupled: the in-plane deformations $w_{x'}(\mathbf{r}')$ and $w_{y'}(\mathbf{r}')$ on the one hand and the out-of-plane displacements and rotations $w_{z'}(\mathbf{r}')$, $\theta_{x'}(\mathbf{r}')$ and $\theta_{y'}(\mathbf{r}')$, on the other hand. The dynamic in-plane deformations are governed by the coupled Navier-equations [10]. Since the Helmholtz equation (1) assumes the acoustic medium to be inviscid, the acoustic pressure only directly influences the out-of-plane dynamic deformations of the structure. Therefore the in-plane equations are not considered further. To describe the dynamic out-of-plane behaviour a various types of plate bending theories are available. The Kirchhoff thin plate bending theory [10] is the most widely known, but the hybrid methodology applies equally well to other available plate bending theories, such as for example the more general Reissner-Mindlin theory [11]. Without loss of generality, the plate bending differential equations can be written as:

$$\left(\mathbf{L_b} - \omega^2 \mathbf{M_b}\right) \left\{ \begin{array}{c} w_{z'}(\mathbf{r}') \\ \theta_{x'}(\mathbf{r}') \\ \theta_{y'}(\mathbf{r}') \end{array} \right\} = \left\{ \begin{array}{c} f_{z'}(\mathbf{r}') \\ m_{x'}(\mathbf{r}') \\ m_{y'}(\mathbf{r}') \end{array} \right\} \quad (3)$$

In this expression, $\mathbf{L_b}$ is a $(3\text{x}3)$ matrix of differential operators, governing the elastic and damping forces in the plate structure. The elements of the $(3\text{x}3)$ matrix $\mathbf{M_b}$ represent the inertial parameters of the structure. The term on the right hand side of (3) represents the distribution of the mechanically applied forces and moments (per unit area) on the structure.

The structural partial differential equation (3) needs to be complemented with appropriate boundary conditions at each point on the edge Γ_s of the structural domain. Two of the possible types of boundary conditions (BCs) are:

$$\begin{array}{ll} \textbf{Kinematic BCs on } \Gamma_d\text{:} & \mathbf{d}(\mathbf{r}') = \bar{\mathbf{d}}(\mathbf{r}') \\ \textbf{Dynamic BCs on } \Gamma_t\text{:} & \mathbf{T}(\mathbf{r}') = \bar{\mathbf{T}}(\mathbf{r}') \end{array} \quad (4)$$

with $\mathbf{d}(\mathbf{r}')$ and $\mathbf{T}(\mathbf{r}')$, respectively, the vector of out of plane deformations and boundary forces. Variables of the form $\bar{\bullet}$ represent prescribed boundary values.

In a coupled vibro-acoustic system, the acoustic pressure field and the structural displacements mutually influence each other along the vibro-acoustic interaction surface Ω_s as follows:

- The vibrations of the plate act as a normal velocity excitation for the fluid in the cavity:

$$R_{va}(\mathbf{r}) = j\omega w(\mathbf{r}') - \frac{j}{\rho_a \omega} \frac{\partial p(\mathbf{r})}{\partial n} = 0 \quad (5)$$

- The acoustic pressure acts as a supplementary load on the structure. Since this load only affects the out-of-plane bending deformation of the plates, the vibro-acoustic interaction translates into an additional load-term in the bending differential equations (3) which is proportional to the acoustic pressure on the 'wetted' surface:

$$\left(\mathbf{L_b} - \omega^2 \mathbf{M_b}\right) \left\{ \begin{array}{c} w_{z'}(\mathbf{r}') \\ \theta_{x'}(\mathbf{r}') \\ \theta_{y'}(\mathbf{r}') \end{array} \right\} = \left\{ \begin{array}{c} f_{z'}(\mathbf{r}') + p(\mathbf{r}') \\ m_{x'}(\mathbf{r}') \\ m_{y'}(\mathbf{r}') \end{array} \right\} \quad (6)$$

2.2 FEM for uncoupled structural problems

The hybrid FE-WB method combines a FE model of the structural part of the problem with an acoustic WB model of the interior cavity. This section describes the basic concepts of the FEM for uncoupled structural problems. The FEM is a well-known simulation technique to model the steady-state dynamic behaviour of complex structures. The technique determines an approximate solution to the problem described by the plate bending equations (3) and the imposed structural boundary conditions (4) by applying the following strategy:

- The entire problem domain Ω_s is discretised into a large, but finite, number of small, non-overlapping elements.
- The FEM approximates the exact solution by a weighted sum of simple (polynomial) shape functions $N_i(\mathbf{r}')$. For each node i in the FE discretisation there is an associated shape function $N_i(\mathbf{r}')$, which has a non-zero value in each

element domain to which nodal degree of freedom (dof) i belongs, while it is zero in all other element domains. For the out of plane displacements $w_{z'}(\mathbf{r}')$, the approximation is written as:

$$w_{z'}(\mathbf{r}') \approx \hat{w}_{z'}(\mathbf{r}') = \sum_{n=1}^{n_k} N_{n,wz'}(\mathbf{r}') a_{n,wz'} = \mathbf{N_{wz'}} \cdot \mathbf{w_{z'}} \quad (7)$$

with n_k the number of nodal dofs in the FE model, $\mathbf{w_{z'}}$ the (n_kx1) vector of unknown weighting coefficients $a_{n,wz'}$ and $\mathbf{N_{wz'}}$ the (1xn_k) vector of shape functions $N_{n,wz'}(\mathbf{r}')$. For the other field variables, similar expansions are applied. In general, the weighting factors $a_{n,i}$ in these expansions represent the unknown nodal deformations.

- The polynomial shape functions are no exact solutions of the governing differential equations and may violate the imposed boundary conditions. The approximation errors are forced to zero in an integral sense by application of a Galerkin weighted residual formulation [1].
- This results in a set of algebraic equations of the form:

$$(\mathbf{K} + j\omega\mathbf{C} - \omega^2\mathbf{M}) \cdot \mathbf{d} = \mathbf{Z} \cdot \mathbf{d} = \mathbf{f_s} \quad (8)$$

with **K**, **C** and **M** the structural stiffness, damping and mass matrices, **Z** the structural dynamic stiffness matrix, **d** the vector containing the unknown nodal structural deformations and $\mathbf{f_s}$ the structural loading vector, which contains contributions from the structural excitations and the dynamic boundary conditions. Solution of (8) yields the deformations in the nodes of the FE discretisation.

The dynamic stiffness matrix **Z** is large, symmetric and sparsely populated and can be decomposed into frequency independent submatrices (**K**, **C**, **M**). These properties allow the use of very efficient solution algorithms to compute the unknown nodal displacements **d**. The use of simple polynomial shape functions to describe the complex dynamic behaviour within the elements, limits the application range of the FEM. A large number of elements is required to control interpolation and pollution errors. A rule of thumb states that between 6 and 10 (linear) finite elements are needed to accurately interpolate a single wavelength of a bending wave [3]. Since physical wavelengths shorten with increasing frequency, a growing number of elements (and dofs) is required, resulting in a rapid increase of the model size. However, a major advantage of the FEM is its versatility regarding geometrical complexity of the problem domain.

2.3 WBM for uncoupled acoustic problems

The hybrid FE-WB method applies the WBM to model the dynamic behaviour of the fluid in the cavity. This section describes the basic concepts of the WBM. The WBM, which is based on an indirect Trefftz approach [5], partitions the entire problem domain V into a small number of large, convex subdomains. Within these subdomains, the dynamic acoustic pressure $p(\mathbf{r})$ is written as a weighted sum of wave functions, which exactly satisfy the Helmholtz equation (1), but which may violate the imposed boundary conditions. A weighted residual formulation is used to force the errors at the boundaries to zero in an integral sense. Solution of the resulting system of algebraic equations yields the contributions of the wave functions in the solution expansion.

2.3.1 Field variable approximation

The acoustic pressure field $p(\mathbf{r})$ within a convex cavity is approximated by a finite solution expansion $\hat{p}(\mathbf{r})$:

$$p(\mathbf{r}) \approx \hat{p}(\mathbf{r}) = \sum_{a=1}^{n_a} \Phi_a(\mathbf{r}) \cdot p_a + \hat{p}_q(\mathbf{r}) = \mathbf{\Phi} \cdot \mathbf{p_a} + \hat{p}_q(\mathbf{r}) \quad (9)$$

with $\mathbf{p_a}$ a (n_ax1) vector of unknown wave function contributions p_a, $\mathbf{\Phi}$ a (1xn_a) vector collecting the wave functions $\Phi_a(\mathbf{r})$. $\hat{p}_q(\mathbf{r}) = \frac{j\rho\omega q}{4\pi} \frac{e^{-jkd(\mathbf{r},\mathbf{r_q})}}{d(\mathbf{r},\mathbf{r_q})}$ is a particular solution of the inhomogeneous Helmholtz equation (1), with $d(\mathbf{r},\mathbf{r_q}) = \sqrt{(x-x_q)^2+(y-y_q)^2+(z-z_q)^2}$ the

distance between a point at coordinates $\mathbf{r}(x,y,z)$ inside the cavity and the acoustic source q.

Desmet [4] proposes the use of the following set of wave functions:

$$\begin{cases} \Phi_r(\mathbf{r}) = \cos(k_{xr}x).\cos(k_{yr}y).e^{-jk_{zr}z} \\ \Phi_s(\mathbf{r}) = \cos(k_{xs}x).e^{-jk_{ys}y}.\cos(k_{zs}z) \\ \Phi_t(\mathbf{r}) = e^{-jk_{xt}x}.\cos(k_{yt}y).\cos(k_{zt}z) \end{cases} \quad (10)$$

In order for the wave functions to be exact solutions of the homogeneous Helmholtz equation, the wave number components in (10) need to satisfy:

$$k_{xi}^2 + k_{yi}^2 + k_{zi}^2 = k^2 \quad (11)$$

Desmet [4] proves that a convergent set of wave functions is obtained if the following limited set is selected from the infinite number of possible wave number sets which satisfy (11):

$$\begin{aligned} (k_{xr},k_{yr},k_{zr}) &= \left(\tfrac{a_1\pi}{L_x}, \tfrac{a_2\pi}{L_y}, \pm\sqrt{k^2-(\tfrac{a_1\pi}{L_x})^2-(\tfrac{a_2\pi}{L_y})^2}\right) \\ a_1 &= 0,1,2,\ldots, \quad a_2 = 0,1,2,\ldots \\ (k_{xs},k_{ys},k_{zs}) &= \left(\tfrac{a_3\pi}{L_x}, \pm\sqrt{k^2-(\tfrac{a_3\pi}{L_x})^2-(\tfrac{a_4\pi}{L_z})^2}, \tfrac{a_4\pi}{L_z}\right) \\ a_3 &= 0,1,2,\ldots, \quad a_4 = 0,1,2,\ldots \\ (k_{xt},k_{yt},k_{zt}) &= \left(\pm\sqrt{k^2-(\tfrac{a_5\pi}{L_y})^2-(\tfrac{a_6\pi}{L_z})^2}, \tfrac{a_5\pi}{L_y}, \tfrac{a_6\pi}{L_z}\right) \\ a_5 &= 0,1,2,\ldots, \quad a_6 = 0,1,2,\ldots \end{aligned} \quad (12)$$

The lengths L_x, L_y and L_z are the dimensions of the (smallest) rectangular bounding box, enclosing the considered subdomain.

A numerical model with a finite number of dofs is constructed by defining an upper bound on parameters $a_1 \ldots a_6$ in Eq.(12) through application of a frequency dependent truncation rule:

$$\frac{n_{a1}}{L_x} \approx \frac{n_{a2}}{L_y} \approx \frac{n_{a3}}{L_x} \approx \frac{n_{a4}}{L_z} \approx \frac{n_{a5}}{L_y} \approx \frac{n_{a6}}{L_z} \geq N \cdot \frac{k}{\pi} \quad (13)$$

Applying this truncation rule results in the use of all wave functions with wavelength larger than or equal to $1/N$ times the physical wavelength at each frequency of interest.

2.3.2 Wave based model

Since the pressure expansion (9) exactly satisfies the governing equation (1), the only error consists of the violation of the imposed boundary conditions. In order to obtain a numerical model for the n_a wave function contributions, this error is minimised in a weighted residual sense, by taking into account the three different types of acoustic boundary error residuals in (2):

$$-\int_{\Omega_p} \frac{j}{\rho_a\omega} \frac{\partial \tilde{p}(\mathbf{r})}{\partial n} \cdot R_p(\mathbf{r}) d\Omega + \int_{\Omega_v} \tilde{p}(\mathbf{r}) \cdot R_v(\mathbf{r}) d\Omega + \int_{\Omega_Z} \tilde{p}(\mathbf{r}) \cdot R_Z(\mathbf{r}) d\Omega = 0 \quad (14)$$

with $\tilde{p}(\mathbf{r})$ arbitrary weighting functions. Applying a Galerkin approach, the latter functions are written in terms of the same basis functions that are used in the field variable expansion (9). Introduction of the field variable expansion (9) and the weighting functions into the residual formulation (14) yields a system of n_a equations in the n_a unknown wave function contributions p_a:

$$\mathbf{A_{aa}} \cdot \mathbf{p_a} = \mathbf{f_a} \quad (15)$$

Solution of this system for the unknown wave function contributions $\mathbf{p_a}$ and substitution of these results in (9) yields an approximation $\hat{p}(\mathbf{r})$ for the acoustic pressure response. The acoustic system matrix $\mathbf{A_{aa}}$ is fully populated with complex elements. Moreover, since the wave functions (10) explicitly depend on the excitation frequency ω, the matrix coefficients need to be recalculated for every excitation frequency. The system matrix cannot be decomposed into frequency-independent submatrices. The major advantage of the WBM is the substantially smaller number of dofs required in comparison to the FEM. This property, combined with the enhanced convergence properties of the method, make the WBM a computationally more efficient simulation technique than the FEM and allow the WBM to be used for vibro-acoustic analysis in the mid-frequency range. The requirement of convexity of the wave based subdomains imposes, however, a limitation to the practical applicability of the method for complex geometries.

2.4 A direct hybrid FE-WB method for coupled vibro-acoustic problems

	FEM	WBM
model size	large	small
solution time	medium/high	low
convergence rate	medium	high
frequency range	low	low, mid
geometrical complexity	high	moderate

Table 1 Model properties of the FEM and the WBM

Table 1 summarises of the characteristic properties of the FEM and the WBM. This table shows that

both techniques are complementary. This forms the basis for the development of a hybrid modelling technique. Section 3 focuses on the vibro-acoustic analysis of an aircraft fuselage. This is a typical application in which the structure itself is composed of thin shells and beam-like frame and longeron components (see figure 3(b)). Even though the WBM could be used to predict structural responses, a wave based model of the fuselage structure would consist of a large number of structural subdomains. As a result, the WBM's computational efficiency is not fully exploited. A FE model is far more suited for this kind of structural problems. The acoustic cavity, on the other hand, is geometrically simple and can be modelled as a single WB subdomain. A FE discretisation of the acoustic domain is possible but needs to be rather fine in the vicinity of the wetted surface, in order to obtain an accurate vibro-acoustic coupling. This results in a large number of acoustic FE dofs.

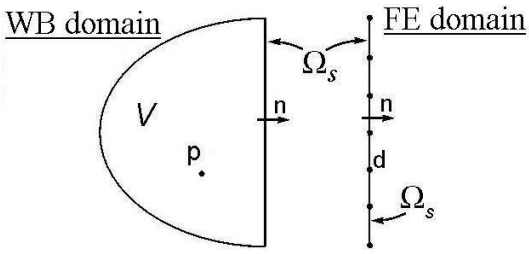

Fig. 2 Direct hybrid FE-WB coupling approach

The velocity continuity conditions (5) and introduction of the pressure loading term in the coupled structural equations describe the mutual interaction between the structural vibrations and the acoustic pressure field. The hybrid FE-WB method uses the same field variable expansions (7) and (9) as the uncoupled techniques to approximate the structural displacements and acoustic pressure. Introduction of the expansions in the coupled equations yields a set of algebraic expressions which directly relate the dofs of both physical domains to each other. Figure 2 represents the direct coupling between the two physical domains. The weighted residual formulation for the FE domain is expanded to take into account the supplementary acoustic pressure loading on the structure. The velocity continuity along the structural-acoustic interface Ω_s is taken into account in the WBM weighted residual formulation (14) by adding the following term:

$$\int_{\Omega_s} \tilde{p}(\mathbf{r}) \cdot R_{va}(\mathbf{r}) d\Omega \tag{16}$$

Combination of the residual formulations for both domains and application of a Galerkin approach yields the following matrix equation for the coupled vibro-acoustic system:

$$\begin{bmatrix} \mathbf{A_{aa}} + \mathbf{C_{aa}} & j\omega\mathbf{C_{as}^T} \\ \mathbf{C_{as}} & \mathbf{Z} \end{bmatrix} \cdot \begin{Bmatrix} \mathbf{p} \\ \mathbf{d} \end{Bmatrix} = \begin{Bmatrix} \mathbf{f_a} + \mathbf{f_{sa}} \\ \mathbf{f_s} + \mathbf{f_{as}} \end{Bmatrix} \tag{17}$$

With $\mathbf{Z}$, $\mathbf{A_{aa}}$, $\mathbf{f_s}$ and $\mathbf{f_a}$ the system matrices and loading vectors from the uncoupled structural (8) and acoustic (15) models. The acoustic-structural and structural-acoustic coupling matrices $\mathbf{C_{as}}$ and $j\omega\mathbf{C_{as}^T}$ describe the mutual vibro-acoustic interaction and $\mathbf{C_{aa}}$ is the acoustic back-coupling matrix. The supplementary loading terms $\mathbf{f_{as}}$ and $\mathbf{f_{sa}}$ result from the acoustic point source q in V.

3 Validation example: Vibro-acoustic modelling of a DC8 fuselage section

3.1 Problem definition

The performance of the hybrid FE-WB methodology is validated through a study of the interior noise inside a section of an aircraft fuselage, as shown in figure 3(a). A two-frame quarter section of the fuselage of a DC8 airplane and the interior acoustic cavity are modelled using the FEM and the hybrid method. The structure is composed of thin skin panels attached to circumferential frames and longitudinal longerons. Figure 3(b) gives an overview of the stiffeners used in the fuselage of a DC8 aircraft. The entire structure is made of aluminium ($E = 70GPa$, $\nu = 0.3$, $\rho_s = 2790kg/m^3$). The geometrical details of the fuselage components are described in [12]. The structure is excited using an excentric point load F (see figure 3(a)). The connection between the excitation point and the fuselage is made through two rigid beams. The imposed structural boundary conditions on the fuselage are shown in figure 3(c). Along the axial edges of the section the axial rotation and the circumferential displacement are zero. At the nodes along the circumferential edge of the fuselage a zero axial displacement is applied. The internal acoustic cavity has the shape of a quarter of a cylinder and is filled with air ($\rho_a = 1.225kg/m^3$, $c = 340m/s$). Along the acoustic boundaries which are not in contact with the structure, rigid wall BCs are imposed, describing the symmetry of the cavity with respect to these planes. The structural components inside the cavity (floors, seats, internal cabin wall...) are not considered.

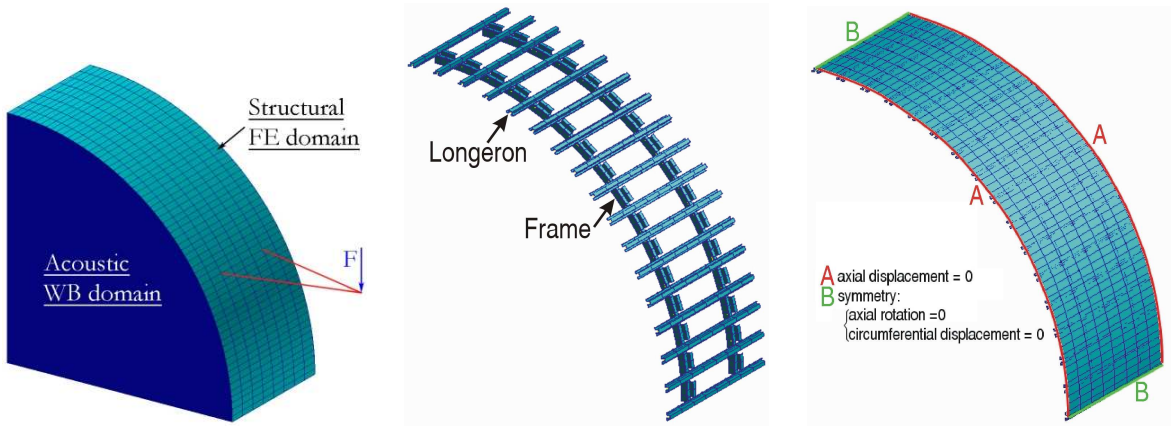

(a) (b) (c)

Fig. 3 Vibro-acoustic DC8 fuselage model, (a) Hybrid model, (b) Stiffener-configuration, (c) Structural boundary conditions

	$dofs_{structure}$ (= #nodes x 6)	$dofs_{acoustic}$ (= #nodes)	h_{max} $[m]$	$f_{6,s}$ $[Hz]$	$f_{10,s}$ $[Hz]$	$f_{6,a}$ $[Hz]$	$f_{10,a}$ $[Hz]$
FE Model 1	586x6 = 3516	11987	0.127	20.5	7.38	446.2	267.7
FE Model 2	1106x6 = 6636	22643	0.0635	82	29.5	892.4	535.4
FE Model 3	3226x6 = 19356	75824	0.0423	184.8	66.7	1341	804.7
FE Model 4	4258x6 = 25548	100089	0.03175	328	118.1	1619	971
FE Reference model	6322x6 = 37932	148617	0.0225	653.2	235.2	2518	1511

Table 2 Properties of the various FE models

3.2 Coupled models

3.2.1 FE models

The structural FE models are built using 4-noded bilinear shell elements attached to cubic 2-noded beam elements, used to model the longerons and frames. Table 2 gives an overview of the different structural models used in the comparison. h_{max} is the length of the longest side of a finite element in the discretisation and $f_{6,s}$ and $f_{10,s}$ indicate the upper frequencies for which the FE models include at least 6 or 10 structural elements per wavelength. The results of the finest discretisation are used as the reference solution. The interior acoustic cavity is represented by a mesh of 8-noded trilinear fluid elements. The details of the acoustic FE models of the cavity are listed in table 2. $f_{6,a}$ and $f_{10,a}$ indicate the maximum frequency up to which the acoustic models are expected to yield accurate results using 6 and 10 elements per wavelength, respectively. MSC.Nastran2004 is used as FE solver.

3.2.2 Hybrid models

The hybrid models use the same structural parts as the pure FE descriptions. The acoustic cavity is modelled by a single acoustic WB domain. By varying the truncation parameter N in (13), each of the structural FE models can be used to create a number of hybrid models with a different number of acoustic WB dofs. The values of the truncation parameters N, used in this validation are given in table 3. The routines to build and solve the hybrid and the associated WB models are implemented in Matlab 6.5. All calculations are performed on a 3GHz Intel-based Linux-system with 1 gigabyte of RAM.

Hybrid model	1	2	3	4	5	6	7
N	0.5	1	1.5	2	2.5	3	4

Table 3 Truncation parameter N for the hybrid models

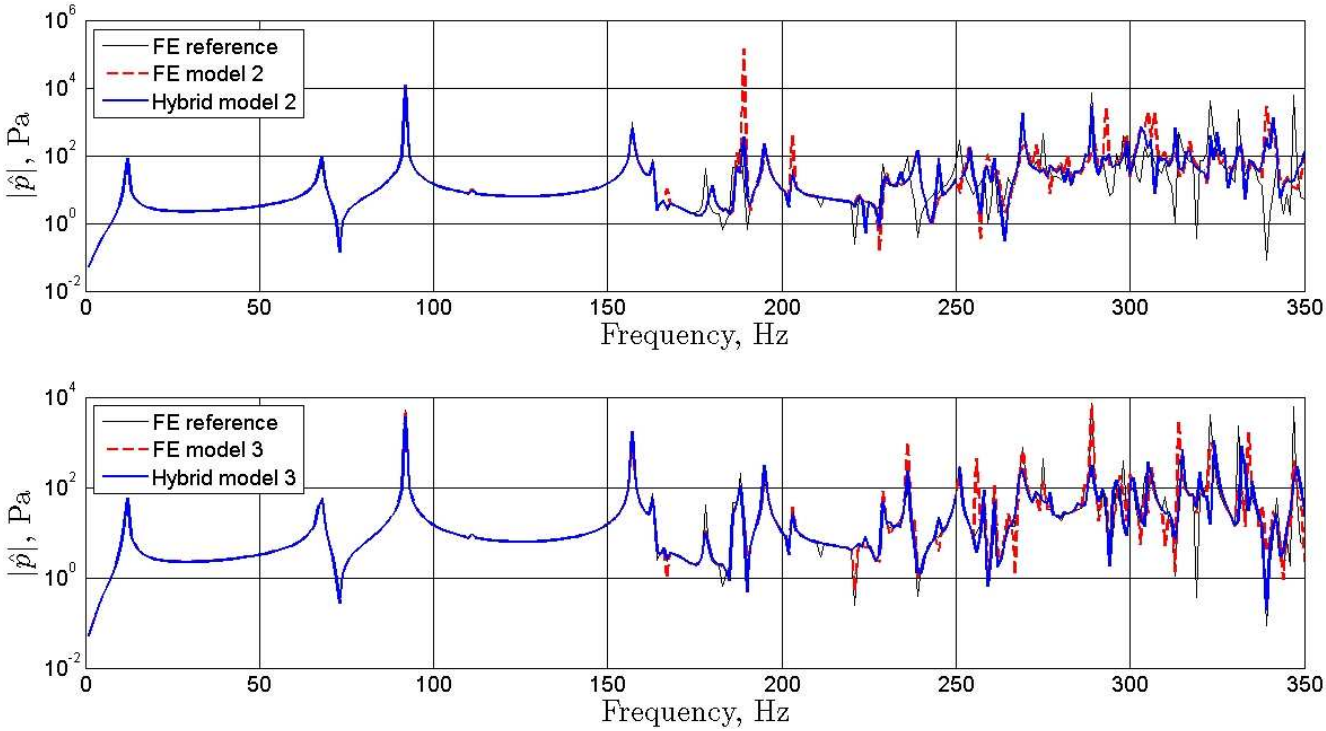

Fig. 5 Acoustic pressure response spectrum, top: structural model 2 (coarse), bottom: structural model 5 (fine)

3.3 Numerical results

To illustrate that the hybrid method accurately describes the vibro-acoustic coupling effects between the fuselage and the internal acoustic cavity, figure 4 shows a color map of the acoustic pressure amplitude at 169*Hz* obtained with a hybrid (right figure) and a FE model (left figure). Both models use the same FE model for the structure (model 3). The number of acoustic dofs in the FE model is 75824, while only 168 acoustic wave functions are used in the hybrid model. The results show a good agreement between both methods.

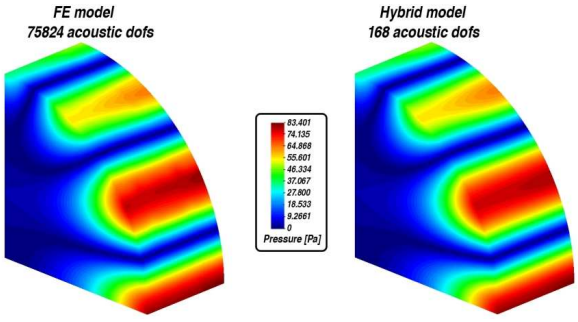

Fig. 4 Pressure amplitude color map at 169*Hz*

Figure 5 gives the pressure amplitude spectrum at a point inside the cavity, calculated with FE and hybrid FE-WB models. The computational loads for the full response calculations are comparable for both models. The top figure shows the pressure response for a relatively coarse structural model (structural model 2). The bottom figure is obtained with a model with a much finer structural discretisation (structural model 3). The results are compared with the FE reference solution (black line). All the models yield the same predictions at low frequencies (up to 175*Hz*). At higher frequencies, the models with a coarser structural part (both pure FE and hybrid FE-WB) exhibit a shift in some of the predicted resonance frequencies. Due to the too coarse structural mesh used in the structural models, the predicted structural wavelengths in the numerical model differ from the real physical bending wavelengths. The errors in the predicted resonance frequencies are a direct result of these so-called numerical dispersion errors [3]. Since both predictions suffer equally from dispersion it is concluded that the structural part of the model determines the dispersion error in this example. At very high frequencies (above 300*Hz*), the coarse models are no longer valid, resulting in incorrect predictions. The models with a fine structural part suffer less from numerical dispersion. Even at higher frequencies both the pure FE and the hybrid model accurately predict the resonance frequencies of the coupled vibro-acoustic system.

In order to compare the computational efficiency of the hybrid method and the FEM, a convergence analysis is performed. The acoustic pressure at $169Hz$ in 20 response points, uniformly distributed inside the acoustic cavity is calculated for all the models described in section 3.2. The average relative prediction error ε_{av} for the acoustic pressure, as defined in (18), and calculation time for each analysis are compared in order to determine the convergence rate for both methods.

$$\varepsilon_{av} = \frac{1}{20}\sum_{j=1}^{20}\varepsilon_j = \frac{1}{20}\sum_{j=1}^{20}\left|\frac{\hat{p}(\mathbf{r_j}) - p_{ref}(\mathbf{r_j})}{p_{ref}(\mathbf{r_j})}\right| \qquad (18)$$

with $\hat{p}(\mathbf{r_j})$ the calculated pressure response and $p_{ref}(\mathbf{r_j})$ a reference acoustic pressure at each of the response locations $\mathbf{r_j}$. In the convergence analysis presented here, the finest FE model is used to obtain the reference solution. Only frequency dependent operations are taken into account in the calculation time. For the FEM only the time needed to solve the system of equations is given. For the hybrid method the time needed to build the WB system matrix and the hybrid coupling matrices as well as the time needed to solve the system of equations are considered. The time to build the FE matrices is not taken into account for the hybrid method, nor for the FEM, since this effort is frequency independent and negligible when a large number of frequencies are considered.

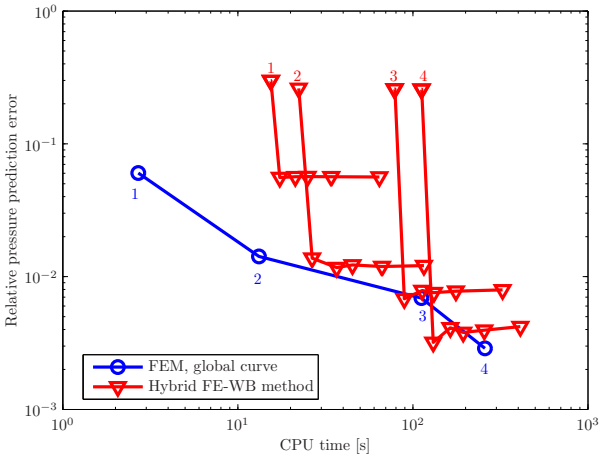

Fig. 6 Individual pressure convergence curves at $169Hz$: relative pressure prediction error as a function of CPU time

Figure 6 compares the convergence rate of the different hybrid models with that of the FE models. The figure contains the global convergence curve for the FEM (o marker) and individual convergence curves for various hybrid models (∇ marker). The global curve for the FEM is obtained by simultaneously refining the structural and acoustic meshes in the model. The numbers along the curve for the FEM indicate which FE model in table 2 was used to calculate the different points. The individual convergence curves for the hybrid models are calculated by combining a fixed structural part with an increasing number of wave functions (using the truncation parameters in table 3). The numbers above each of the curves indicate which structural FE model is used to obtain the hybrid convergence curve. The convergence curves show that, as the number of wave functions increases, the prediction accuracy of the hybrid models increases steadily until some saturation is reached where the error remains constant. All the hybrid convergence curves have an elbow shape. The saturation level is determined by the density of the structural FE mesh and it is similar to the error for a pure FE model with the same structural part. The prediction accuracy increases for both the FEM and the hybrid FE-WB method when the structural FE model is refined.

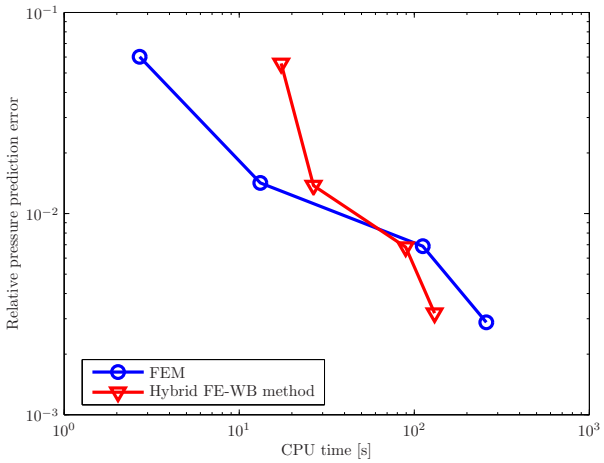

Fig. 7 Global pressure convergence curves at $169Hz$

The individual curves for the hybrid models in figure 6 can be combined to obtain a global convergence curve for the hybrid method by interconnecting the elbow points for each of the curves. Figure 7 shows the global convergence curves for the FEM (o marker) and hybrid method (∇ marker). The FEM results are identical to the ones given in figure 6 and give the increase in the pressure prediction accuracy with respect to the increase in calculation time when the structural and acoustic FE models are refined simultaneously. The blue triangle curve gives the results for four hybrid models. Each triangle represents a hybrid

model with a different structural FE part. The number of wave functions used in the hybrid models is equal to the minimal number needed to obtain convergence of the models (elbow points in figure 6). The figure shows that the global convergence curve for the hybrid method is steeper than that of the FE models (a unit increase in calculation time due to a model refinement results in a higher gain in the average prediction accuracy for the hybrid FE-WB method than for the FEM). This shows the enhanced convergence properties of the hybrid method. For denser structural meshes a higher accuracy is obtained in less time. This allows for faster prediction calculations or further refinement of the model to obtain a higher prediction accuracy within the same calculation time.

4 Conclusions

This paper describes a newly developed hybrid FE-WB modelling technique for steady-state vibro-acoustic problems. In many coupled problems a complex structure interacts with a geometrically simple acoustic cavity. The motivation for the hybrid approach is the combination of the advantages of both techniques in a 'best of two worlds'-methodology. The complex structural part is described in great detail by the geometrically versatile FEM. The application of the WBM for the acoustic part results in favourable convergence properties of the method. The hybrid method presented in this paper couples the structural FE and acoustic WB models by directly enforcing the velocity continuity on the WB part and by directly imposing the acoustic pressure loading on the structural FE part.

A comparison between the FEM and the hybrid FE-WB method is made based on a vibro-acoustic study of a DC8 fuselage section. The results illustrate that the prediction accuracy of the hybrid models increases as the number of wave functions increases, until saturation is reached and the prediction error remains constant at a level similar to that of the pure FE predictions. The density of the structural FE model determines the maximum prediction accuracy. Especially for denser structural meshes, the hybrid method leads to a higher accuracy in less computation time. These results illustrate the potential of the hybrid FE-WB method as a powerful tool for the prediction of the dynamic behaviour of coupled vibro-acoustic systems.

Future research includes a further enhancement of the computational efficiency of the technique. Furthermore, the possibility of enforcing the vibro-acoustic coupling in an indirect manner and the use of modally reduced structural FE models for the structural part of the problem will be explored.

References

[1] O. C. Zienkiewicz and R. L. Taylor, *The finite element method - Volume 1: Basic formulation and linear problems*, Butterworth Heinemann, Oxford, pp. 124-127, 2000.

[2] C. A. Brebbia, J. C. F. Telles, and L. C. Wrobel, *Boundary element techniques - Theory and application in engineering*, Springer-Verlag, Berlin, 1984.

[3] P. Bouillard and F. Ihlenburg, "Error estimation and adaptivity for the finite element method in acoustics: 2d and 3d applications," *Computer Methods in Applied Mechanics and Engineering*, vol. 176, pp. 147–163, January 1999.

[4] W. Desmet, *A wave based prediction technique for coupled vibro-acoustic analysis*, Ph.D. thesis, Katholieke Universiteit Leuven, Leuven, 1998.

[5] E. Trefftz, "Gegenstück zum ritzschen verfahren," in *Proceedings of the 2nd International Congress of Applied Mechanics*, Zürich, Switzerland, 1926, pp. 131–137.

[6] W. Desmet, B. Van Hal, P. Sas, and D. Vandepitte, "A computationally efficient prediction technique for the steady-state dynamic analysis of coupled vibro-acoustic systems," *Advances in Engineering Software*, vol. 33, pp. 255-283, 2003.

[7] B. Van Hal, W. Desmet, D. Vandepitte, and P. Sas, "A coupled finite element - wave based approach for the steady state dynamic analysis of acoustic systems," *Journal of Computational Acoustics*, vol. 11(2), pp. 255–283, 2003.

[8] C. Vanmaele, W. Desmet, and D. Vandepitte, "A direct hybrid finite element-wave based prediction technique for the steady-state dynamic analysis of two-dimensional solids," *CDROM Proceedings of the 12th International Congress on Sound and Vibration (ICSV12)*, 2005.

[9] P.M. Morse and K.Uno. Ingard, *Theoretical acoustics*, McGraw-Hill, New York, 1968.

[10] A. Leissa, *Vibration of plates*, Acoustical Society of America, 1973.

[11] O. C. Zienkiewicz and R. L. Taylor, *The finite element method - Volume 2: Solid mechanics*, Butterworth Heinemann, Oxford, pp. 111-215, 1997.

[12] Michael C.Y. Niu, *Airframe structural design*, Conmilit Press Ltd, Hong Kong, pp. 384-390, 1988.